

THERMAL ANALYSES OF RUBIDIUM AND CESIUM OXALATE MONOHYDRATES

RYŌKOU ITO *, YOSHIO MASUDA ** *** and YOSHIO ITO *

* *Department of Chemistry, Faculty of Science, Niigata University, Niigata 950-21 (Japan)*

** *Chemistry Division, General Education Department, Niigata University, Niigata 950-21 (Japan)*

(Received 20 July 1987)

ABSTRACT

Thermal analyses of rubidium and cesium oxalate monohydrates were carried out by means of thermogravimetry, differential thermal analysis and differential scanning calorimetry together with powder X-ray diffraction analysis. Both the oxalate monohydrates $\text{Rb}_2\text{C}_2\text{O}_4 \cdot \text{H}_2\text{O}$ and $\text{Cs}_2\text{C}_2\text{O}_4 \cdot \text{H}_2\text{O}$ belong to the monoclinic crystal system with cell dimensions of $a = 9.68$, $b = 6.35$, $c = 11.09$ Å and $\beta = 109.4^\circ$ at 20°C and $a = 10.19$, $b = 6.67$, $c = 11.44$ Å and $\beta = 108.0^\circ$ at 20°C , respectively. Three crystallographic modifications (phases I, II and III) were identified for both dehydrated oxalates. The crystals of $\text{Rb}_2\text{C}_2\text{O}_4$ and $\text{Cs}_2\text{C}_2\text{O}_4$ in phase I have an orthorhombic unit cell with $a = 3.69$, $b = 6.60$ and $c = 13.94$ Å at 330°C and $a = 3.82$, $b = 6.84$ and $c = 14.44$ Å at 330°C , respectively.

Heating the crystals of $\text{Rb}_2\text{C}_2\text{O}_4$ in phase I to 380°C , transforms the specimen into phase II belonging to the orthorhombic crystal system with lattice parameters $a = 4.56$, $b = 6.53$ and $c = 9.49$ Å at 385°C . At temperatures above 388°C , the crystals of phase II transform into phase III which belongs to the tetragonal crystal system with $a = 4.59$ and $c = 6.67$ Å at 405°C . Both the phase transitions $\text{I} \rightarrow \text{II}$ and $\text{II} \rightarrow \text{III}$ are reversible. The crystals in phase III begin to decompose at around 450°C .

The crystals of $\text{Cs}_2\text{C}_2\text{O}_4$ in phase I also transformed reversibly into phase II at 400°C , and into phase III at 451°C . The crystals in phase II have orthorhombic unit cell with $a = 4.77$, $b = 6.82$ and $c = 9.95$ Å at 440°C , and in phase III a tetragonal unit cell with $a = 4.66$ and $c = 7.04$ Å at 465°C . The crystals in phase III decomposed above 470°C .

The dehydration of both oxalate monohydrates proceeded as a phase boundary reaction. The decomposition of $\text{Rb}_2\text{C}_2\text{O}_4$ also proceeded as a phase boundary reaction. However, the decomposition behavior of $\text{Cs}_2\text{C}_2\text{O}_4$ was characteristic of a homogeneous first-order reaction since the specimen melted during the decomposition.

Activation energies of the dehydration and the decomposition were determined for both oxalates.

*** Author to whom correspondence should be addressed

INTRODUCTION

Several studies have been carried out on the thermal decomposition of metal oxalates. The thermal analyses of alkali metal oxalates have also been studied by several investigators [1–8]. Dollimore and Griffith [1] have studied the differential thermal analyses of sodium and potassium oxalates in nitrogen and oxygen. They showed that their decomposition to the carbonate is endothermic in nitrogen, but exothermic in oxygen. The kinetic study of the thermal decomposition of lithium oxalate to the carbonate has been also carried out by Dollimore and Tinsley [2]. They showed that the reaction occurred with an increase in the surface area, followed by extensive sintering, and its kinetics followed a phase boundary mechanism. Higashiyama and Hasegawa [7] have found the three crystallographic modifications of the anhydrous potassium salt by means of differential thermal and thermogravimetric analysis together with the X-ray diffraction method. Adams and Ramdas [8] have studied the kinetics of the thermal dehydration and deperhydration of some alkali metal hydrates and perhydrates. However, the thermal analyses of rubidium and cesium oxalates have been sparsely studied.

In the course of thermal analysis of alkali metal oxalates, we found [9] that anhydrous rubidium and cesium oxalates have three different crystallographic phases. In the present study, to obtain further detailed information on both the oxalates, their thermal behavior was investigated by means of thermogravimetry (TG), differential thermal analysis (DTA), differential scanning calorimetry (DSC) and the X-ray powder diffraction method.

EXPERIMENTAL

Materials

Rubidium and cesium oxalates were prepared from the reaction between oxalic acid and respective carbonates, by the method previously described [10]. The anhydrous oxalates were highly hygroscopic. On standing overnight at room temperature, the anhydrous oxalates changed to the respective oxalate monohydrate.

Measurements

Thermogravimetric (TG) and differential thermal analytic (DTA) curves were obtained simultaneously with differential thermal microbalances, a Rigaku-Denkī TG-DTA M 8075 and a Shinku-Riko TGD-5000 RH. About 20 mg of powder specimen were weighed in a platinum crucible, and α -alumina was used as a reference material. Derivative thermogravimetric

(DTG) curves were obtained by the method described previously [11,12] Differential scanning calorimetric curves were recorded with a Shinku-Riko DSC-1500 M/L About 10 mg of specimen were placed in an aluminum crucible, and α -alumina was used as reference material This instrument was calibrated with the heats of melting of indium ($\Delta H = 3.27 \text{ kJ mol}^{-1}$, 156.5°C) and zinc ($\Delta H = 6.57 \text{ kJ mol}^{-1}$, 419.6°C) [13]

Powder X-ray diffractograms were obtained with a Rigaku-Denkı diffractometer, RAD-rA, equipped with a standard high temperature sample holder $\text{Cu } K_\alpha$ radiation, nickel filter and a graphite monochromator were used in all measurements In X-ray diffraction measurements at a high temperature, the specimen was heated at a rate of 2°C min^{-1} and cooled at $-2^\circ\text{C min}^{-1}$ After attaining a given temperature, the specimen was kept at constant temperature for 1 h Diffraction patterns were taken at a step width of 0.02° The diffraction lines could be indexed by a microcomputer (Sharp MZ-2000)

The specimen released gaseous products with increasing temperature The gaseous products evolved were collected in syringes at various temperatures, and 2 cm^3 of each gas collected was analyzed by a Shimadzu Gas Chromatograph GC-4B equipped with a thermal conductivity detector The separation column was a $2 \text{ m} \times 5 \text{ mm}$ i.d. stainless steel tube packed with 60–80 mesh WG-100 (purchased from Gasukuro Kogyo) The column and the detector were kept at 50°C , and helium was used as a carrier gas at a flow rate of $30 \text{ cm}^3 \text{ min}^{-1}$

IR absorption spectra were measured from 250 to 4000 cm^{-1} in KBr disks with a Hitachi 295 spectrophotometer

RESULTS AND DISCUSSION

Thermal analyses of $\text{Rb}_2\text{C}_2\text{O}_4 \cdot \text{H}_2\text{O}$ and $\text{Cs}_2\text{C}_2\text{O}_4 \cdot \text{H}_2\text{O}$

TG and DTA curves of $\text{Rb}_2\text{C}_2\text{O}_4 \cdot \text{H}_2\text{O}$ in a flowing dry nitrogen atmosphere ($70 \text{ cm}^3 \text{ min}^{-1}$) are shown in Fig 1 The TG curve shows that the dehydration took place in the temperature range 84 – 145°C , and the weight loss observed (6.5%) was equal to that required by theory for dehydration In the DTA curves, the endothermic peak associated with dehydration was recognized at 133°C After dehydration, overlapping two endothermic peaks were found at 384 and 392°C in the DTA curve, but no weight loss corresponding to these peaks was found The endothermic decomposition of $\text{Rb}_2\text{C}_2\text{O}_4$ began at around 450°C , and appeared to be complete at 635°C

The TG and DTA curves of $\text{Cs}_2\text{C}_2\text{O}_4 \cdot \text{H}_2\text{O}$ (Fig 1) were similar to those of $\text{Rb}_2\text{C}_2\text{O}_4 \cdot \text{H}_2\text{O}$ The dehydration took place in the temperature range 35 – 76°C After the dehydration, two endothermic peaks observed at 404 and 455°C were not accompanied by a corresponding weight loss The

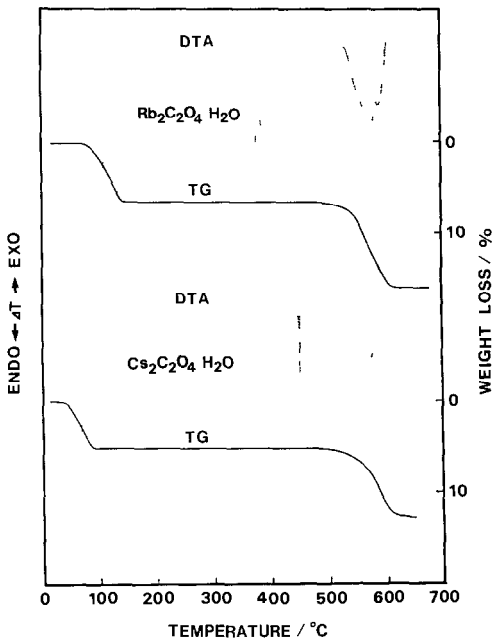


Fig 1 TG (solid line) and DTA (broken line) for the thermal analysis of $\text{Rb}_2\text{C}_2\text{O}_4 \cdot \text{H}_2\text{O}$ and $\text{Cs}_2\text{C}_2\text{O}_4 \cdot \text{H}_2\text{O}$ in a dry nitrogen flow atmosphere Heating rate, $10^\circ\text{C min}^{-1}$

decomposition of this anhydrous product took place in the temperature range $440\text{--}635^\circ\text{C}$. These findings suggest the existence of phase transformations in both the anhydrous compounds

Phase transformations of $\text{Rb}_2\text{C}_2\text{O}_4$ and $\text{Cs}_2\text{C}_2\text{O}_4$

To obtain further information about the two endothermic phase transitions observed in the temperature range between dehydration and decomposition, DSC measurements and powder X-ray diffraction analyses were examined in detail at high temperatures

When the DSC measurement of $\text{Rb}_2\text{C}_2\text{O}_4$ was carried out at a heating rate of 2°C min^{-1} , the two peaks (P_1 and P_2) were separated clearly (Fig 2). On cooling the specimen preheated to 430°C , two exothermic peaks (P'_2 and P'_1) appeared. If the specimen was cooled to any temperature below 360°C and was reheated, it behaved like the initial sample. The values of enthalpy changes for these phase transitions on heating and on cooling, were determined from the peak areas of DSC curves and are shown in Table 1. It is noteworthy that the absolute values of heats of the phase transitions P_1 and P_2 are almost equal to those of P'_1 and P'_2 , respectively. This finding suggests that the phase transitions are reversible.

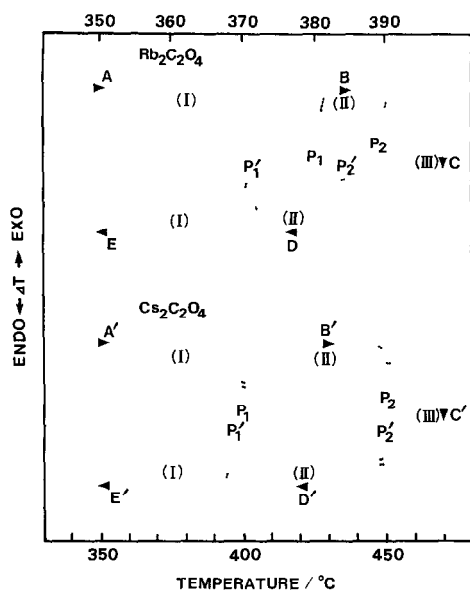


Fig 2 Heating and cooling DSC of $\text{Rb}_2\text{C}_2\text{O}_4$ and $\text{Cs}_2\text{C}_2\text{O}_4$. Symbols A–E and A'–E' show the temperature at which the X-ray diffraction patterns were measured. A, 330, B, 385, C, 405, D, 380, E, 330, A', 330, B', 440, C', 470, D', 440, and E', 330 °C. Symbols (I)–(III) show the phases.

Figure 3 shows the X-ray powder diffraction pattern (F) of $\text{Rb}_2\text{C}_2\text{O}_4 \cdot \text{H}_2\text{O}$ at room temperature and those (A–E) of $\text{Rb}_2\text{C}_2\text{O}_4$ measured at various temperatures. The crystal of $\text{Rb}_2\text{C}_2\text{O}_4 \cdot \text{H}_2\text{O}$ has a monoclinic system with cell dimensions $a = 9.68$, $b = 6.35$, $c = 11.09$ Å and $\beta = 109.4^\circ$ at 20 °C from indexing its diffraction lines. The results are consistent with the data reported ($a = 9.662$, $b = 6.350$, $c = 11.088$ Å and $\beta = 109.4^\circ$) by Pedersen [14].

After dehydration, $\text{Rb}_2\text{C}_2\text{O}_4$ crystals show the diffraction pattern in Fig 3A. The diffraction lines can be indexed on the assumption that $\text{Rb}_2\text{C}_2\text{O}_4$ crystal has an orthorhombic unit cell with lattice constants $a = 3.69$, $b = 6.60$ and $c = 13.94$ Å at 330 °C. This phase is stable below 370 °C and is called

TABLE 1

Enthalpy changes for phase transformation of $\text{Rb}_2\text{C}_2\text{O}_4$ and $\text{Cs}_2\text{C}_2\text{O}_4$

	ΔH (kJ mol ⁻¹)			
	Heating		Cooling	
	P ₁	P ₂	P' ₁	P' ₂
$\text{Rb}_2\text{C}_2\text{O}_4$	6.7 ± 0.1	3.9 ± 0.1	-6.5 ± 0.1	-3.8 ± 0.0
$\text{Cs}_2\text{C}_2\text{O}_4$	2.8 ± 0.1	1.8 ± 0.1	-2.7 ± 0.1	-1.9 ± 0.0

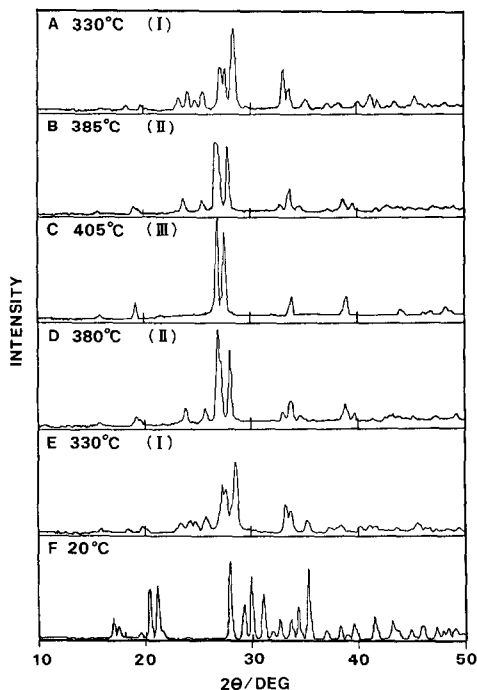


Fig 3 X-Ray diffraction patterns of $\text{Rb}_2\text{C}_2\text{O}_4$ and $\text{Rb}_2\text{C}_2\text{O}_4 \cdot \text{H}_2\text{O}$ See Fig 2 for symbols A–E and (I)–(III) Symbol F shows $\text{Rb}_2\text{C}_2\text{O}_4 \cdot \text{H}_2\text{O}$

phase I When the crystals of $\text{Rb}_2\text{C}_2\text{O}_4$ in phase I were heated and held at 385°C for 1 h, the specimen shows a different diffraction pattern from that of phase I (Fig 3B) The diffraction lines could be indexed on the basis of an orthorhombic cell with lattice constants $a = 4.56$, $b = 6.54$ and $c = 9.49$ Å at 385°C The phase is stable in the temperature range 382 – 387°C and is called phase II When phase II was further heated and held at 405°C , the specimen shows a new diffraction pattern (Fig 3C) The diffraction lines can be indexed on the assumption that the crystal has a tetragonal unit cell with lattice constants $a = 4.59$ and $c = 6.67$ Å at 405°C This phase is stable above 390°C until decomposition, and is called phase III When the specimen preheated at 405°C was cooled to 380°C and held for 1 h, it gives similar diffraction lines to those of phase II (Fig 3D) When the specimen was cooled to 330°C and held for 1 h, it also gives a similar diffraction pattern to that of phase I (Fig 3E) These findings confirm that the above phase transformations $\text{I} \rightarrow \text{II} \rightarrow \text{III}$ are reversible

The thermal behavior of $\text{Cs}_2\text{C}_2\text{O}_4 \cdot \text{H}_2\text{O}$ was similar to that of $\text{Rb}_2\text{C}_2\text{O}_4 \cdot \text{H}_2\text{O}$ Two reversible transformations were also confirmed by means of DSC measurements and X-ray diffraction analyses at high temperatures (Figs 2 and 4) The crystallographic data of $\text{Cs}_2\text{C}_2\text{O}_4 \cdot \text{H}_2\text{O}$ and $\text{Cs}_2\text{C}_2\text{O}_4$ have not yet been reported Their X-ray diffraction profiles were similar to those of

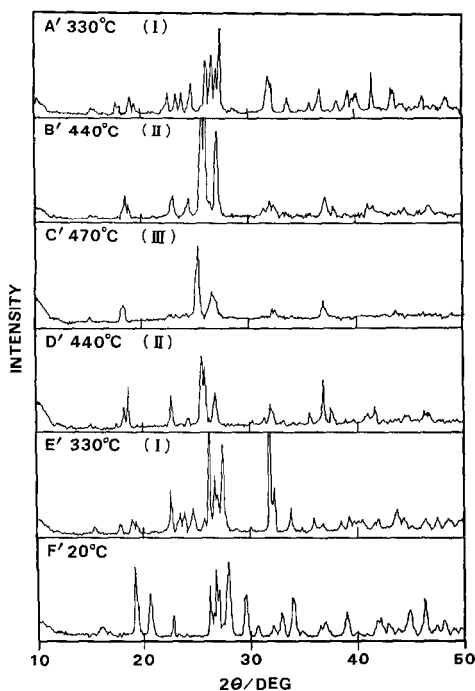


Fig 4 X-Ray diffraction patterns of $\text{Cs}_2\text{C}_2\text{O}_4$ and $\text{Cs}_2\text{C}_2\text{O}_4 \cdot \text{H}_2\text{O}$ See Fig 2 for symbols A'–E' and (I)–(III) Symbol F' shows $\text{Cs}_2\text{C}_2\text{O}_4 \cdot \text{H}_2\text{O}$

$\text{Rb}_2\text{C}_2\text{O}_4 \cdot \text{H}_2\text{O}$ and $\text{Rb}_2\text{C}_2\text{O}_4$, respectively. The powder X-ray diffraction lines of $\text{Cs}_2\text{C}_2\text{O}_4 \cdot \text{H}_2\text{O}$, could be indexed on the assumption that the crystal has a monoclinic unit cell with lattice constants shown in Table 2. After the dehydration, phase I appeared (Fig 4A') and it transformed into phase II at 401°C (Fig 4B'). The crystals in phase II transformed into phase III at temperatures higher than 450°C (Fig 4C'). When the specimen in phase III was cooled and held at 440°C for 1 h, it gave a similar diffraction profile to that of phase II (Fig 4B'). Further, when the specimen was cooled and held at 330°C for 1 h, it also showed similar X-ray diffraction lines to those of phase I (Fig 4E'). Therefore, these two transformations are reversible. The crystal structures of the three crystal phases were estimated from indexing the X-ray diffraction lines, and are shown in Table 2. The comparison of the cell dimensions of $\text{Rb}_2\text{C}_2\text{O}_4$ with those of $\text{Cs}_2\text{C}_2\text{O}_4$ shows that the latter are slightly larger in each phase (Table 3) although the cell dimensions in phase II and III are compared at different temperatures. This seems to be due to the difference in the ionic radius of cesium and rubidium ions.

In the first transformation (I \rightarrow II), the changes in lattice parameters are considerable, i.e. the length of the *a*-axis lengthens, whereas that of the *c*-axis shortens. The second transformation (II \rightarrow III) appears to be from orthorhombic to tetragonal. However, changes in lattice parameters are not

TABLE 2

Unit cell dimensions

	Phase			
	Monohydrate	(I)	(II)	(III)
<i>Rb₂C₂O₄</i>				
Cell dimension	$a = 9.68 \text{ \AA}$ $b = 6.35 \text{ \AA}$ $c = 11.09 \text{ \AA}$ $\beta = 109.4^\circ$	$a = 3.69 \text{ \AA}$ $b = 6.60 \text{ \AA}$ $c = 13.94 \text{ \AA}$	$a = 4.56 \text{ \AA}$ $b = 6.54 \text{ \AA}$ $c = 9.49 \text{ \AA}$	$a = 4.59 \text{ \AA}$ $c = 6.67 \text{ \AA}$
Temperature (°C)	20 Monoclinic	330 Orthorhombic	385 Orthorhombic	405 Tetragonal
<i>Cs₂C₂O₄</i>				
Cell dimension	$a = 10.19 \text{ \AA}$ $b = 6.67 \text{ \AA}$ $c = 11.44 \text{ \AA}$ $\beta = 108.0^\circ$	$a = 3.82 \text{ \AA}$ $b = 6.84 \text{ \AA}$ $c = 14.44 \text{ \AA}$	$a = 4.77 \text{ \AA}$ $b = 6.82 \text{ \AA}$ $c = 9.95 \text{ \AA}$	$a = 4.66 \text{ \AA}$ $c = 7.04 \text{ \AA}$
Temperature (°C)	20 Monoclinic	330 Orthorhombic	440 Orthorhombic	470 Tetragonal

large compared with those of the I → II transformation. These seem to be consistent with the fact that the enthalpy change measured for the first transformation is larger than that for the second (Table 1). The phase transformation and the changes of lattice parameters with increasing temperatures suggest that the phase III is a stage in the course of the phase transitions from the orthorhombic system (being stable at lower temperatures) to the cubic system, because it is unstable at higher temperatures.

No transformations were seen in the thermal analyses of $\text{Li}_2\text{C}_2\text{O}_4$ and $\text{Na}_2\text{C}_2\text{O}_4$ which have a monoclinic crystal system [15,16]. The crystals decompose to their respective carbonates directly.

Higashiyama and Hasegawa [7] have investigated the thermal transformation of $\text{K}_2\text{C}_2\text{O}_4$. They found that an orthorhombic phase was stable at room temperature, and the phase transformed irreversibly into a tetragonal phase.

TABLE 3

Ratios of cell dimensions

Axis	$\frac{\text{Cs}_2\text{C}_2\text{O}_4}{\text{Rb}_2\text{C}_2\text{O}_4}$	$\frac{\text{H}_2\text{O}}{\text{H}_2\text{O}}$	$\frac{\text{Cs}_2\text{C}_2\text{O}_4 \text{ (I)}}{\text{Rb}_2\text{C}_2\text{O}_4 \text{ (I)}}$	$\frac{\text{Cs}_2\text{C}_2\text{O}_4 \text{ (II)}}{\text{Rb}_2\text{C}_2\text{O}_4 \text{ (II)}}$	$\frac{\text{Cs}_2\text{C}_2\text{O}_4 \text{ (III)}}{\text{Rb}_2\text{C}_2\text{O}_4 \text{ (III)}}$
	<i>a</i>	1.05		1.04	1.05
<i>b</i>	1.05		1.04	1.04	
<i>c</i>	1.03		1.04	1.06	1.06

at 381°C. They also showed that the tetragonal phase transformed reversibly into a new phase when it was cooled to temperatures below 215°C. However, the result from our re-examination shows that it does not agree with their result, and the thermal behavior of $K_2C_2O_4$ is extremely complicated. The thermal transformation of $K_2C_2O_4$ should be re-examined, and the details of thermal transformations of $K_2C_2O_4$ will be reported in a future work.

Thermal decomposition

The TG, DTA and derivative thermogravimetric (DTG) curves of $Rb_2C_2O_4$ are shown in Fig 5, together with the evolved gas analysis (EGA) curve for its thermal decomposition in a flowing dry nitrogen atmosphere. The observed weight loss (10.7%) was consistent with that expected (10.8%) on the basis of the following equation

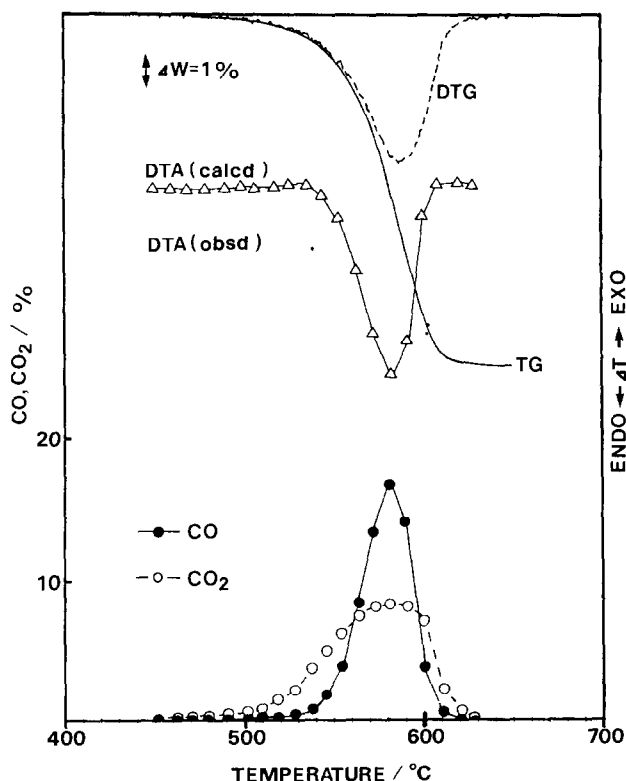
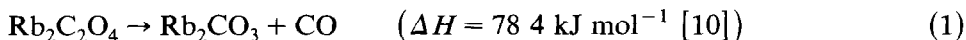
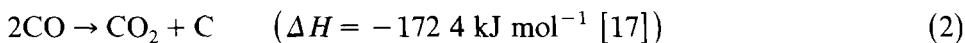


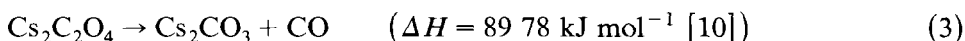
Fig 5 TG, DTG, DTA and evolved gas analyses for thermal decomposition of $Rb_2C_2O_4$ in a dry nitrogen flow atmosphere. Heating rate, $10^\circ\text{C min}^{-1}$.

The analysis of the gas evolved showed that the decomposition occurs with almost simultaneous evolution of CO_2 and CO at 450°C . The ratio of CO_2 to CO was high at the initial stage of decomposition, and varied with increasing temperature. The overall ratio was 1.02. A gray residue due to dispersed carbon was obtained, and the following disproportionation of CO is suggested



A slight and broad exotherm at around 535°C is probably due to this exothermic disproportionation. In Fig. 5, the experimental DTA curve is compared with that simulated by consideration of the enthalpy changes of reactions (1) and (2). The agreement between the curves confirms reactions (1) and (2). The apparent exothermic peak at 585°C in the experimental DTA curve could not be found in the simulated curve. The slight exotherm at 610°C seems to correspond to the crystallization of the decomposition product Rb_2CO_3 .

The thermal decomposition of $\text{Cs}_2\text{C}_2\text{O}_4$ took place analogously to that of $\text{Rb}_2\text{C}_2\text{O}_4$ according to the equation



A slight sharp endothermic peak was observed at 585°C on the DTA curve, and the rate of decomposition changed clearly at this temperature (Fig. 6). Microscopic observation of the specimen of $\text{Cs}_2\text{C}_2\text{O}_4$ at elevated temperatures showed that the specimen melted at this temperature. The findings suggest that this endothermic peak consists of the two peaks corresponding to decomposition and melting.

The evolution of CO_2 suggests the disproportionation of CO . The overall ratio of CO_2 to CO (1.47) is somewhat larger than that of $\text{Rb}_2\text{C}_2\text{O}_4$.

Kinetic analysis

The dehydration and the decomposition of both the oxalates were analyzed kinetically by the method described previously [11,12]. The dehydration of $\text{Rb}_2\text{C}_2\text{O}_4 \cdot \text{H}_2\text{O}$ and $\text{Cs}_2\text{C}_2\text{O}_4 \cdot \text{H}_2\text{O}$ was found to be a two-dimensionally phase-boundary-controlled reaction [18,19]. The values of the activation energies were 76.4 and 25.7 kJ mol^{-1} , respectively. These values correspond to their dehydration temperature. The value for $\text{Rb}_2\text{C}_2\text{O}_4 \cdot \text{H}_2\text{O}$ is smaller than that (247 kJ mol^{-1}) reported by Adams et al. [8]. Their experiment was carried out in a static air atmosphere, whereas ours was in dry nitrogen flow. It is known that the rate of dehydration is considerably influenced by the atmospheric conditions, and the difference may be due to this.

The decomposition of $\text{Rb}_2\text{C}_2\text{O}_4$ occurred as a phase boundary reaction [18,19], and the value of activation energy obtained was 271.8 kJ mol^{-1} . On the other hand, the decomposition of $\text{Cs}_2\text{C}_2\text{O}_4$ occurred as a first-order

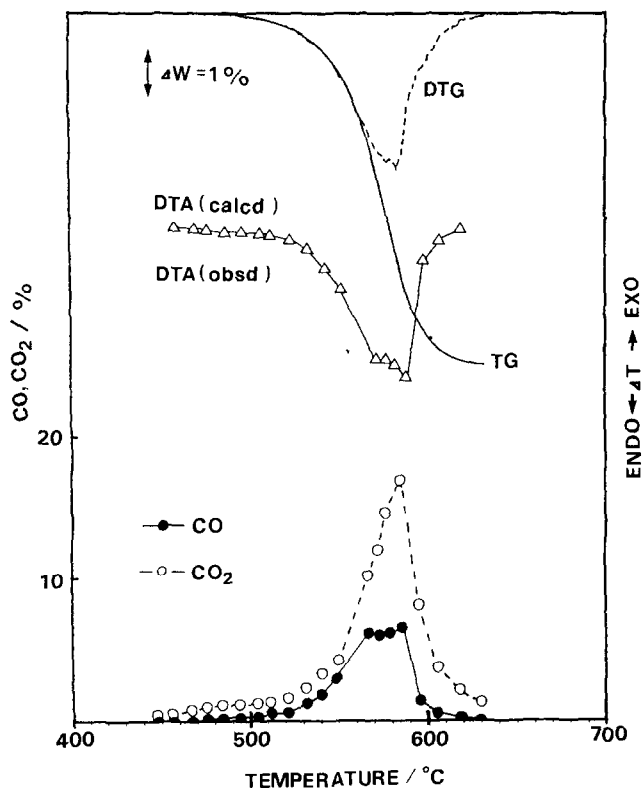


Fig 6 TG, DTG, DTA and evolved gas analyses for thermal decomposition of $\text{Cs}_2\text{C}_2\text{O}_4$ in a dry nitrogen flow atmosphere Heating rate, $10^\circ\text{C min}^{-1}$

reaction It seems reasonable that because $\text{Cs}_2\text{C}_2\text{O}_4$ melts during the decomposition, its decomposition has homogeneous kinetics The value for activation energy was $304.9 \text{ kJ mol}^{-1}$

ACKNOWLEDGMENT

The authors wish to thank Mr. H Minagawa of Analytical Instrument Laboratory, Niigata University, for the high temperature X-ray powder diffraction analyses

REFERENCES

- 1 D Dollimore and D L Griffith, *J Therm Anal*, 2 (1970) 229
- 2 D Dollimore and D Tinsley, *J Chem Soc (A)*, (1971) 3043
- 3 H A Papazian, P J Pizzolato and J A Patrick, *J Am Ceram Soc*, 54 (1971) 250
- 4 K O Hartman and I C Hisatsune, *J Phys Chem*, 71 (1961) 392

- 5 I A Kahwa and A M Mulokozi, *J Therm Anal*, 22 (1981) 61
- 6 I A Kahwa and A M Mulokozi, *J Therm Anal*, 24 (1982) 265
- 7 T Higashiyama and S Hasegawa, *Bull Chem Soc Jpn*, 44 (1971) 1727
- 8 J M Adams and V Ramdas, *J Chem Soc Dalton Trans*, (1980) 269
- 9 R Ito, Y Ito and Y Masuda, 21st Meeting of the Society of Calorimetry and Thermal Analysis, Japan, October 1985, Sapporo Preprint, p 86
- 10 Y Masuda, H Miyamoto, Y Kaneko and K Hirose, *J Chem Thermodynam*, 17 (1985) 159
- 11 Y Masuda, Y Ito, R Ito and K Iwata, *Thermochim Acta*, 99 (1986) 159
- 12 Y Masuda, Y Ito, R Ito and K Iwata, *Thermochim Acta*, 102 (1986) 263
- 13 The Chemical Society of Japan (Ed), *Kagaku Binran Kisohen II (Handbook of Chemistry)*, Maruzen, Tokyo, 3rd edn, 1984, p 270
- 14 B F Pedersen, *Acta Chem Scand*, 19 (1965) 1815
- 15 B Beagley and R W H Small, *Acta Crystallogr*, 17 (1964) 183
- 16 G A Jeffrey and G S Parry, *J Am Chem Soc*, 76 (1954) 5283
- 17 The Chemical Society of Japan (Ed), *Kagaku Binran Kisohen II (Handbook of Chemistry)*, Maruzen, Tokyo, 3rd edn, 1984, p 306
- 18 J H Sharp, G W Brindley and B N N Achar, *J Am Ceram Soc*, 6 (1969) 379
- 19 S F Hulbert, *J Br Ceram Soc*, 6 (1969) 11